DOR: 20.1001.1.2322388.2020.8.2.4.5

Research Paper

Age-Hardening Behavior and the Related Changes in a Silver-Copper-Palladium Alloy

Morteza Hadi[1*], Iman Ebrahimzadeh[2], Omid Bayat[3]

1- Assistant professor, Metallurgy and Materials Engineering Department, Golpayegan University of Technology, Golpayegan 87717-65651, Iran
2- Assistant professor, Advanced Materials Research Center, Department of Materials Engineering, Najafabad Branch, Islamic Azad University, Najafabad, Iran
3- Assistant professor, Department of Metallurgy and Materials Engineering, Hamedan University of Technology, Hamedan 65155-579, Iran

ARTICLE INFO

Article history:

Received 17 October 2019
Accepted 15 December 2019
Available online 28 April 2020

Keywords:

Ag-Cu-Pd alloys
Age-hardening
Scanning electron microscopy
X-ray diffraction

ABSTRACT

Age-hardening behavior and related changes were studied to elucidate the hardening mechanism of an Ag–Cu–Pd alloy by Differential Scanning Calorimetry (DSC), hardness test, X-ray diffraction (XRD), scanning electron microscopic (SEM) observations and energy dispersive spectrometer (EDS). The results showed that hardness of the alloy was raised to 90% and 68% of its solution state value by isothermal aging at 300 ˚C and 400 ˚C, respectively. However, aging at 500 ˚C led to a decrease in the hardness of the alloy. Moreover, while age hardening at 300 ˚C occurred due to coherency strains between the (111) plane of Ag-rich and the (111) plane of Cu_3Pd phases, the mechanism of aging at 400 ˚C was the formation of Cu_3Pd superlattice with the $L1_2$-type crystal structure. In contrast, reduction of Cu_3Pd phase and formation of Cu solid solution decreased hardness during aging at 500ºC.

[*]**Corresponding Author:**
E-mail address: Morteza.hadi@gmail.com

1. Introduction

Ag-Cu alloys with different percentages of Ag and Cu, have various applications such as conductor wires, brazing alloys, dental clinics and source/drain electrodes for thin-film transistors; they also act as metastable alloys [1-8]. The Ag-Cu Phase system contains three phases: liquid phase with no miscibility gap, an Ag-rich phase solid solution phase with an fcc structure with the maximum solubility of 14.1 at.% Cu, and a Cu-rich solid solution phase with, again, the fcc structure with the maximum solubility of 4.9 at.% Ag [9].

Addition of palladium to Ag-Cu alloys could improve the properties of the Ag-Cu eutectic alloy as well as the admixed amalgam. This improvement includes reduced current density during anodic polarization and reduced release rates of metal ions (particularly mercury) during free corrosion [9]. Meanwhile, the application of the Ag–Cu eutectic filler slightly alloyed with noble Pd elements can effectively improve resistance to the galvanic corrosion of the Ti–STS dissimilar joints [2,11]. Also, Ag-Cu-Pd brazing alloy, particularly the alloy with the composition of Ag-20%Cu-15%Pd, is widely used in the vacuum brazing of electronic devices and air craft gas turbine engines [12-14].

On the other hand, it is well known that the mechanical properties of Ag-Cu-based alloys can be improved by age-hardening [1,9]. In such silver alloys, since the slight changes in the atomic ratio can lead to the formation of the different phases, the age-hardening mechanism is directly determined by the alloy composition [1,10]. Several works have been dedicated to the hardening of Ag-Cu-Pd alloys with Au addition [15-18]. However, age hardenability and hardening mechanism of Ag-Cu-Pd alloys are not clear. In the present study, Ag-20%Cu-15%Pd alloy was used to examine the age-hardening behavior and phase transformation.

2. Experimental procedure

A small ingot of about 300 gr in weight with the composition of Ag-20Cu-15Pd (wt %) was arc-melted in an argon atmosphere using a laboratory setup (ALD), which could ensure a high accuracy in obtaining the desired composition. The ingot was remelted six times to improve its homogeneity. The chemical composition of the as-cast alloy was verified by EDS analysis. Cast plates were rolled to plate-like shapes of 5 mm thickness. The specimens were solution-treated at 800 ˚C for 30 min under argon atmosphere, and rapidly quenched into the ice brine system to prevent the occurrence of equilibrium. Differential Scanning Calorimetry (DSC) was applied to the solution-treated sample from room temperature to 650 ˚C using a DSC apparatus (NETZSCH STA 409 PC/PG). DSC was performed at a heating rate of 10 ˚C min^{-1} under an argon atmosphere. Samples were isothermally aged in the temperature ranges of 300–550 ˚C, for various periods of time, in a molten salt bath (25%KNO_3 +30%KNO_2 +25%$NaNO_3$ +20% $NaNO_2$) used for temperatures between 150 ˚C to 550 ˚C; then they were quenched into the ice brine.

Hardness measurements were made using a Vickers micro-hardness tester (Zuick) with the load of 300 gf and the dwell time of 10 Seconds. Hardness results were obtained as the average values of five measurements. Phase identification of selected samples was carried out using an X-ray diffractometer operating at 30 kV; Cu K_α radiation was used with the diffraction angle (2θ) from 30 to 90 and scanning speed of $1^\circ S^{-1}$. The specimens were examined at 20 kV using a scanning electron microscope (VEGA\TESCAN-LMU). Composition of the regions and phases in the samples were analyzed with an energy dispersive spectrometer (EDS).

3. Results

The microstructure of as-cast alloy is shown in figure 1. As can be seen, dendritic microstructure was formed due to the rapid cooling conditions of the water-cooled copper crucible in VAR furnace. The SEM image with higher magnification shows that the phase between dendrites has a quasi-eutectic structure. SEM micrograph of the alloy after solution-treatment at 800 ˚C for 30 min is shown in figure 2. light regions in EDS analysis shows a silver-rich phase (indicated by A), while the dark regions represent a copper-rich one (indicated by B). However, a small amount of silver was found in the copper phase, and a small amount of copper was observed in the silver one. Although palladium atoms were present in both phases, the results showed that this element was preferentially segregated into the copper-rich phase. These results are in agreement with previous reports focusing on the accumulation of palladium atoms in the Cu-rich phase [10].

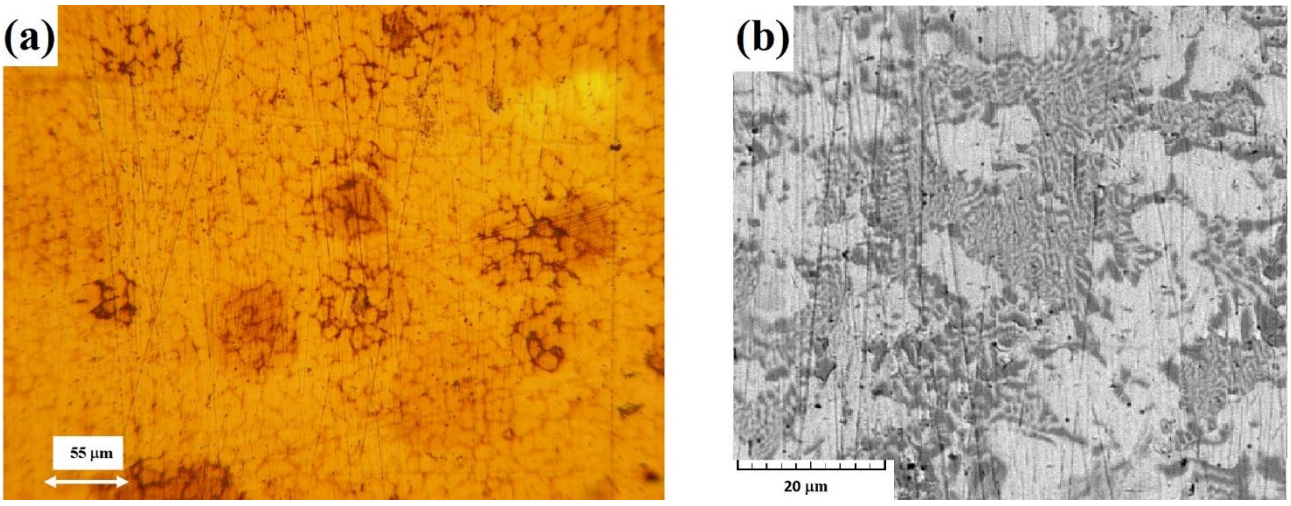

Fig. 1. (a) Optical and (b) BSE-SEM images of as-cast specimen

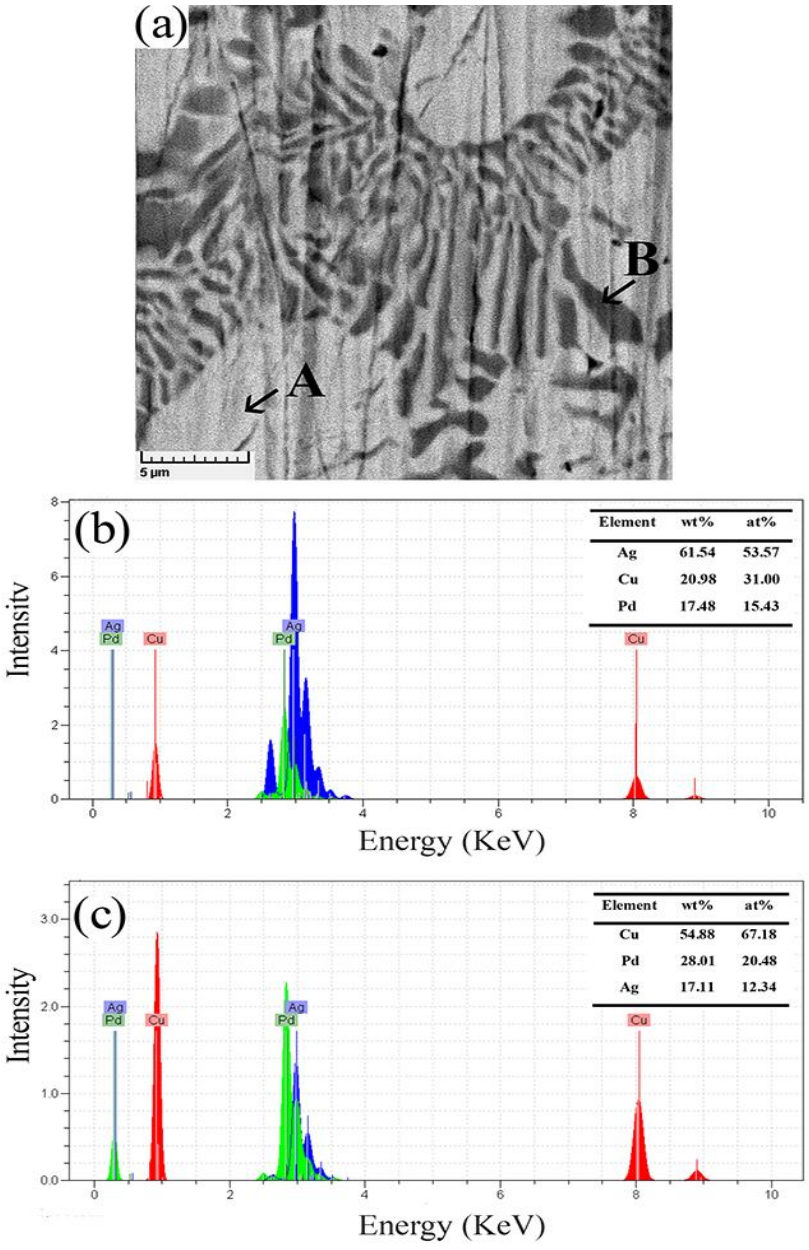

Fig. 2. (a) SEM micrograph of the Ag-Cu-Pd alloy after solution-treatment at 800 ◦C for 30 min, (b) EDS of the region indicated by A, and (c) EDS of the region indicated by B.

XRD pattern of Ag-20Cu-15Pd alloy in solution treated condition is shown in figure 3. Two phases detected in this pattern are Ag solid solution phase and Cu_3Pd ordered phase. Accordingly, since the XRD results showed just two Ag-rich and Cu_3Pd phases in the solution-treated specimen, the gray regions in figure 2 are assumed to be the Cu_3Pd phase. Therefore, the existence of the Ag peak in the EDS of gray regions is supposed to be the result of spectral interferences and spectral background or solution of small amounts of Ag atoms in the Cu_3Pd structure.

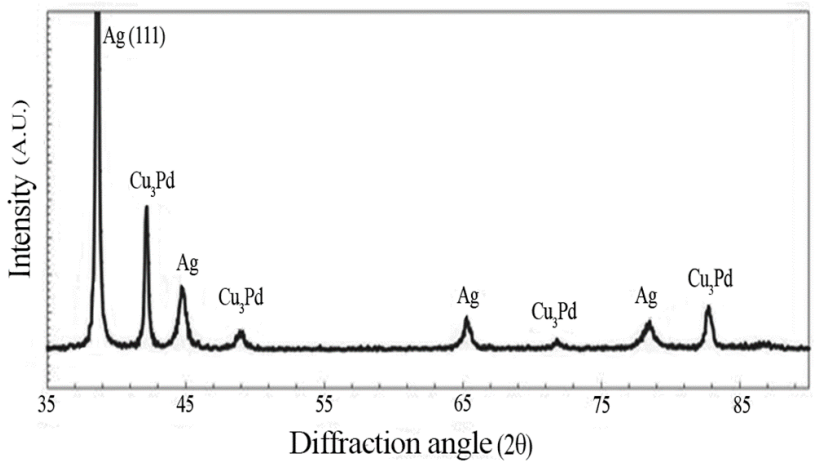

Fig. 3. XRD patterns of the specimen solution-treated at 800°C for 30 min.

Figure 4 shows the DSC curve for heating the solution-treated specimen from room temperature to 650 °C. One exothermic peak at 392 °C and one endothermic peak at 497 °C were observed in the studied temperature range. It could be seen from the figure that two types of transformation had occurred between room temperature and 650 °C. These transformations cause important structural changes to be discussed later.

Figure 5 shows the isochronal age-hardening curves of the specimens solution-treated at 800 °C for 30 min and then aged at 300, 350, 400, 450, 500, and 550 °C for 1200 and 6000 seconds. These results show apparent age-hardenability at the aging temperatures of 300 °C and 400 °C. Since the DSC curve (figure 4) demonstrates two transformations at approximately 400 and 500 °C, the isothermal age-hardening curves at 300, 400 and 500 °C are considered to evaluate the age-hardenability of the alloy.

Hardness variations of the alloy during the aging process at 300, 400, and 500 °C are shown in figure 6. By increasing the aging time at 300 °C, the hardness of the alloy increases with little slope, but over the interval from 600 to 6000 seconds, hardness enhances remarkably.

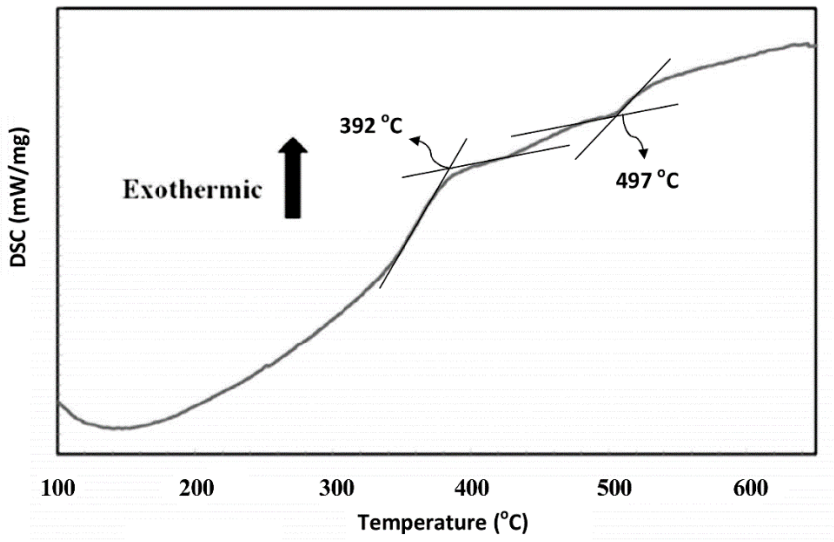

Fig. 4. DSC curve obtained by heating the solution-treated specimen from room temperature to 600 °C. Heating rate was 10 °Cmin^{-1}.

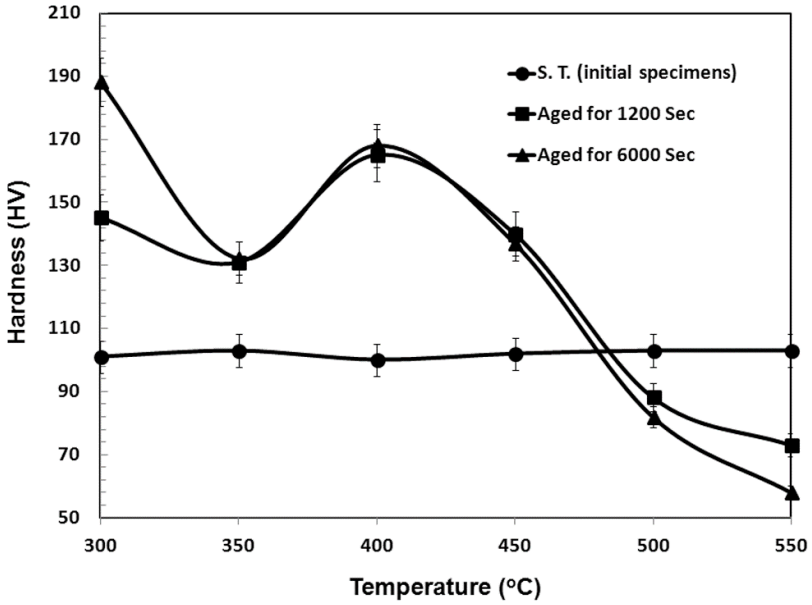

Fig. 5. Isochronal age-hardening curves of the solution treated alloy and the specimens aged in the temperature ranges of 300–550 ˚C for 1200 and 6000 Seconds.

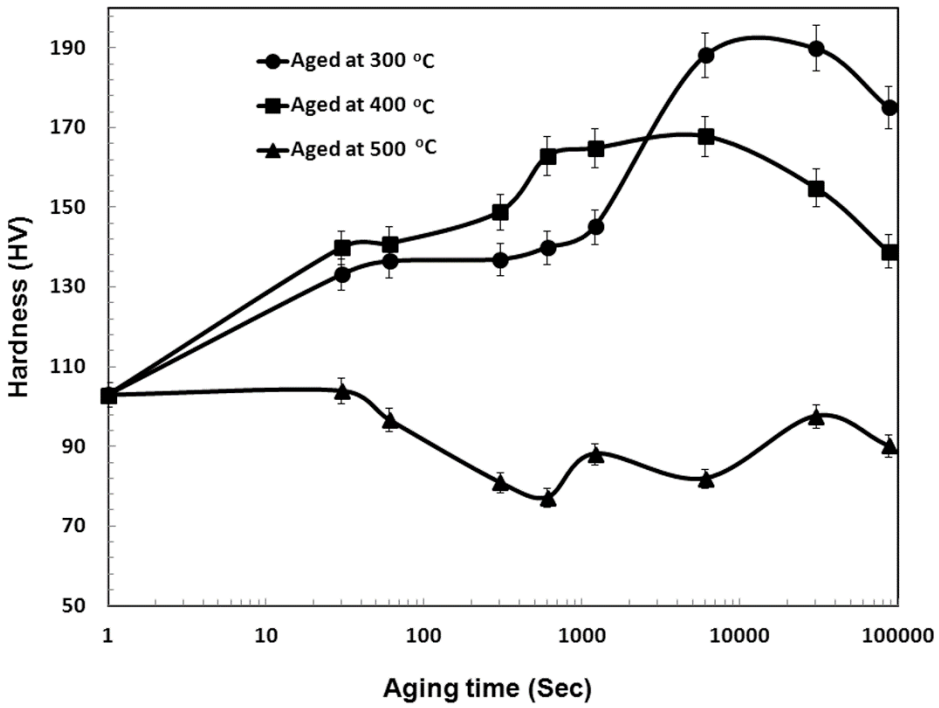

Fig. 6. Isothermal age-hardening curves of the specimen alloy aged at 300, 400 and 500 ˚C.

To investigate the reason for this remarkable hardness difference, two samples aged for 600 and 6000 seconds were studied by XRD analysis. Obtained results are shown in figure 7. As can be seen, related peaks of the Ag-rich phase were shifted to the lower angles, and peaks corresponding to the Cu_3Pd phase were not changed with the increasing aging time.

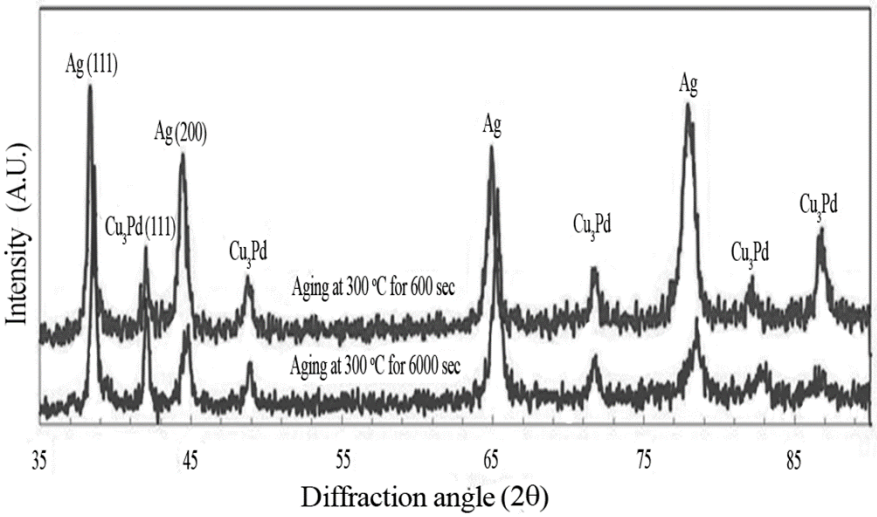

Fig. 7. XRD patterns of the specimens aged at 300 ◦C for 600 and 6000 Seconds.

Contribution of phase transformation to increase of hardness was compared in the two phases by detecting the variations in the full width half maximum (FWHM). Figure 8 shows the variations in the FWHM values with aging time for the plane (111) of the silver-rich phase and the plane (111) of the Cu_3Pd phase. As can be seen, the FWHM values were increased with aging time in both phases suggesting changes in coherency might have occurred. For more details, microstructures of the specimens aged at 300 ◦C for 600 and 6000 seconds were studied by SEM+EDS (figure 9).

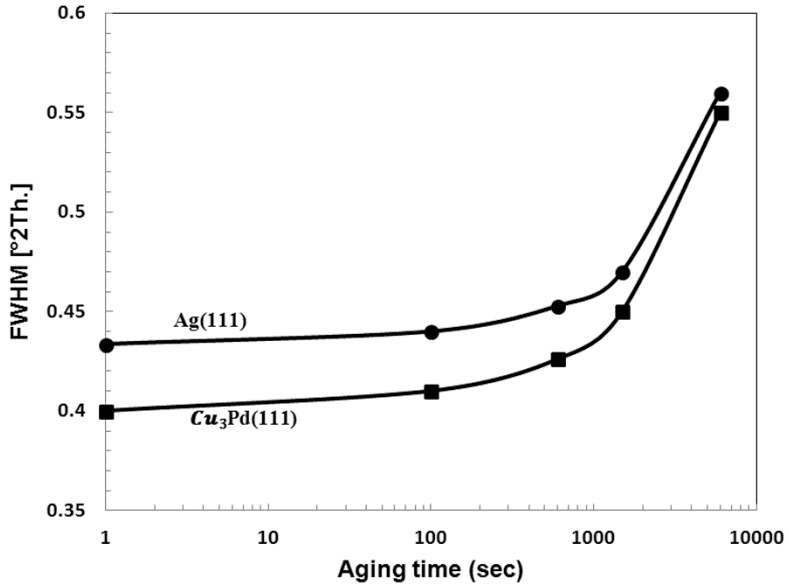

Fig. 8. Variations of the FWHM as measured from the superimposed (111) diffraction peak of the Ag-rich and Cu_3Pd phases at 300 ◦C.

Comparison of the silver-rich phase composition in these alloys with the solution treated specimen (figure 2-(b)) revealed that the weight percent of copper and palladium are decreased with aging time. These results are in accordance with the results of the XRD study. Therefore, on the basis of FWHM studies and SEM/EDS observation, the main reason for increased hardness during aging at 300 ◦C was the egression of copper and palladium atoms from the silver-rich phase and the formation of the Cu_3Pd phase with coherent boundary.

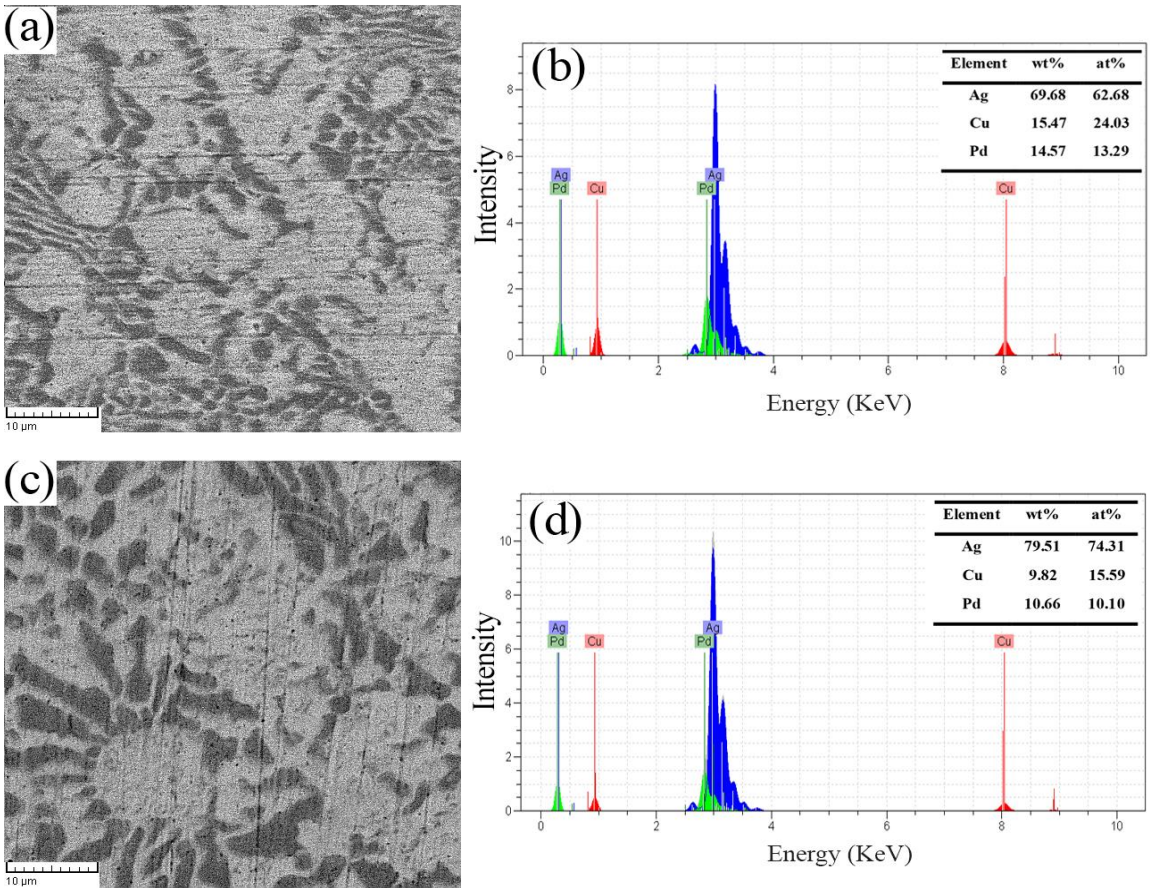

Fig. 9. SEM micrograph and EDS from the light regions of the specimen aged at 300 ºC for 600 seconds (a,b), and for 6000 seconds (c,d).

Also, hardness variations of the alloy during the aging process at 400 ˚C are shown in figure 6. According to this curve, the hardness of the alloy is increased during aging at 400 ˚C. The hardness increment of the samples aged at 400 ˚C was less than that of aged at 300 ˚C. X-ray diffraction analysis of the solution treated sample and the specimens aged at 400 ˚C for 1200 seconds are presented in figure 10. As can be seen from this figure, a new peak at 2θ=36.3 was detected in the pattern of the aged specimen. This peak, which had not been observed in the samples aged at other temperatures, is (011) superlattice peak of the Cu_3Pd phase. It should be noted that all Cu_3Pd peaks that have been observed were fundamental peaks. In most of the regular alloys, superlattice reflections were not visible. Since the atomic numbers of Cu and Pd are 29 and 46, respectively, the difference in the atomic scattering factor is high. Therefore, the intensity of the superlattice reflection is visible.

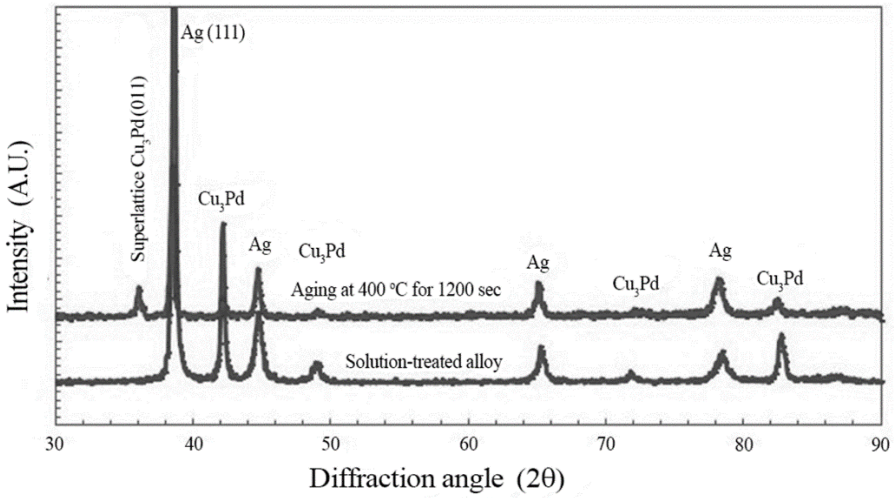

Fig. 10. XRD patterns of the solution-treated alloy and the specimen aged at 400 ºC for 1200 Seconds.

Meanwhile, variations of hardness with aging time at 500 ˚C for Ag-Cu-Pd alloy are indicated in Figure 6. It can be seen that aging of alloy at 500 ˚C lead to the reduction of hardness. X-ray diffraction analysis of the solution treated sample and the specimens aged at 500˚C for 1200 seconds can depicted in figure 11. On the basis of DSC result, there was the possibility of phase transformation at 500˚C (figure 4). By comparing the X-ray diffraction analysis of these two samples, it could be seen that Cu_3Pd peaks disappear or decrease in terms of their intensity during aging at 500 ºC. On the other hand, some new peaks were detected in the XRD pattern. These peaks are related to the copper-rich phase. It seemed that the Cu_3Pd regular phase might have disappeared at 500˚C. Also, the corresponding peaks of CuO and AgO were detected in the X-ray diffraction analysis of the samples aged at temperatures higher than 500 ˚C indicating oxidation due to being maintained at a high temperature for a long time.

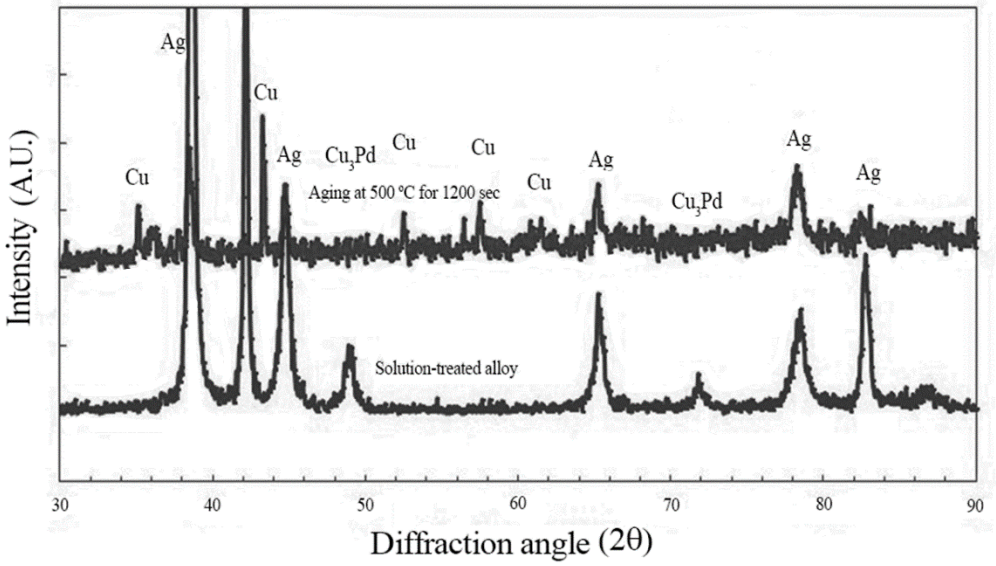

Fig. 11. XRD patterns of the solution-treated alloy and the specimen aged at 500 ºC for 1200 Seconds.

4. Discussion

The first point regarding the age-hardening results is related to the structural changes occurred during aging at 300 ºC. As shown in Figure 6, the shift of Ag peaks to the lower angles reveals that the distance between the crystalline planes in the Ag-rich phase is increased. This could be explained by the fact that copper, silver, and palladium are all possess an fcc structure; among them silver has the largest lattice parameter (0.4086 nm), while copper has the smallest (0.3615 nm) and palladium has a lattice parameter value (0.3890 nm) between silver and copper. Increase in the lattice parameter of the Ag phase is due to the removal of copper and palladium from the Ag-rich phase. It seemed that there is a tendency for palladium separation from the Ag-rich phase. It has been reported that this kind of portioning could occur during casting of the Ag-Cu-Pd alloy containing 10%wt Pd [10,19].

According to Figure 8, FWHM of the (111) plane of Ag and Cu_3Pd was increases by aging time which could have been caused by the increasing of coherency strain after the egression of copper and palladium from the silver-rich phase. This parameter increased the hardness of the Ag-Cu-Pd alloy during aging at 300 ˚C, particularly in the time range of 600 to 6000 seconds. (Figure 6). It seems. that after the egression of copper and palladium from the silver-rich phase, the formation of the fine particles of Cu_3Pd in the silver-rich phase at (111) planes with coherent boundary is possible. Such a hardness increase due to the coherency strains has been commonly reported in the studies addressing the age-hardening mechanisms of some dental alloys [16-22]. In fact, the broadening of diffraction peaks provides evidence of the formation of strains in the lattice structure which leads to the increase of hardness.

On the other hand, variations of the hardness during aging at 400˚C (Figure 6) and detection of peaks corresponding to the (011) superlattice in the XRD patterns of the aged samples (Figure 10) suggested that the formation of superlattice structure could be the main reason of hardening. It has been reported that the hardness could be increased in the ordered alloys by the formation of superlattice structure [23-27]. It seems reasonable because in the alloy aged at 400 ˚C for 1200 Sec, the Cu_3Pd superlattice has the $L1_2$-type crystal structure. However, in the solution-treated alloy, the Cu_3Pd has a periodic APB structure. As shown in Figure 10, the intensity of the

fundamental peaks of Cu_3Pd was reduced during aging. By comparing the intensity of superlattice and fundamental peaks, it could be concluded that a high percentage of the Cu_3Pd phase during aging at 400 ˚C is transformed to the $L1_2$-type crystal structure. Therefore, these results confirm that the exothermic peak at 393˚C (Figure 4) is related to the formation of the superlattice Cu_3Pd.

In the same way, with regard to aging at 500 ˚C, it could be concluded from the XRD (Figure 11) and DSC analysis (Figure 4) that the endothermic peak at 497 ˚C is corresponded to the removal of the Cu_3Pd ordered phase and formation of the copper-rich phase. As summarized in table 1, while changing in the coherency of the second phase was the reason of the hardness increase at 300 ºC, the formation of Cu_3Pd superlattice and the Cu-rich phase could be the reason of hardness variations at 400 and 500 ºC, respectively.

Table 1. Aging behavior of Ag-Cu-Pd alloys investigated in this research.

Aging Temperature	Aging Mechanism
300 ˚C	coherency strains between the (111) plane of Ag-rich and the (111) plane of Cu_3Pd
400 ˚C	Formation of Cu_3Pd superlattice with the $L1_2$-type crystal structure
500 ˚C	Dissolution of the Cu_3Pd phase and formation of the Cu phase

5- Conclusions

In the present study, the hardening mechanism and the related changes of a solution treated Ag-20Cu-15Pd alloy were investigated and the following results were obtained.

1. The alloy showed remarkable age-hardenability at the temperature of 300 ˚C and 400 ˚C. The results suggested that aging at these temperatures could lead to the increase of 90 H.V. and 68 H.V. increases in hardness, respectively.
2. Age-hardening mechanism at 300 ˚C was one of coherency strains between the (111) plane of Ag-rich and the (111) plane of Cu_3Pd.
3. The Cu_3Pd superlattice with the $L1_2$-type crystal structure was formed by aging at 400 ˚C.
4. Dissolution of the ordered Cu_3Pd phase and the formation of the Cu-rich solid solution phase by aging at 500˚C resulted in the decrease of hardness.

References

[1] J. Lin, L. Meng, “Effect of aging treatment on microstructure and mechanical properties of Cu–Ag alloys”, J. Alloy and compd., Vol. 454, 2008, pp. 150–155.

[2] M.C. Vera, J. Martinez-Fernandez, M. Singh, V. Casalegno, C. Balagna, and J. Ramirez-Rico, “Microstructure and thermal conductivity of Si-Al-CO fiber bonded ceramics joined to refractory metals”, Materials Letters, Vol. 276, 2020, pp 128203.

[3] J. Hu, M. Xie, Y. Chen, J. Fang, and Y. Yang, “Structure, energy and electronic properties of Ag/Cu/M (M= Ni, Pd) interfaces: A first principles study”, Computational Materials Science, Vol. 169, 2019, pp 109-133.

[4] Venkateswaran, T., Xavier, V., Sivakumar, D., Pant, B., Jayan, P.K. and Ram, G.J., 2019. Brazing of Martensitic Stainless Steel to Copper Using Electroplated Copper and Silver Coatings. Journal of Materials Engineering and Performance, 28(2), pp.1190-1200.

[5] H. Kim, K.H. Baik, J. Cho, et al., “High-reflectance and thermally stable Ag-Cu alloy p-Type reflectors for GaN-based light-emitting diodes”, IEEE Photonics Tech. L., Vol. 19, 2007, pp. 336-338.

[6] J. Zhang, M. Liang, Q. Hu, F. Ma, Z. Li, Y. Wang, L. Wang, and S. Zhang, “Cu@ Ag nanoparticles doped micron-sized Ag plates for conductive adhesive with enhanced conductivity”, International Journal of Adhesion and Adhesives, 2020, p.102657.

[7] Banhart J, Ebert H, Kuentzler R, et al. Electronic properties of single-phased metastable Ag-Cu alloys. Phys. Rev. 1992; B46:9968-9975.

[8] S. Tardieu, D. Mesguich, A. Lonjon, F. Lecouturier-Dupouy, N. Ferreira, G. Chevallier, A. Proietti, C. Estournès, and C. Laurent, “High Strength-High Conductivity Silver Nanowire-Copper Composite Wires by Spark Plasma Sintering and Wire-Drawing for Non-Destructive Pulsed Fields”, IEEE Transactions on Applied Superconductivity, Vol. 30(4), 2020, pp.1-4.

[9] P.R. Subramanian, J.H. Perepezko, “The Ag-Cu (Silver-Copper) System” J. Phase Equilib., Vol. 14, 1993, pp. 62-75.

[10] K.I. Chen, J.H. Lin, C.P. Ju, “Microstructure and Segregation Behavior of Palladium in Silver-Copper-Palladium Alloys”, J. Dent. Res., Vol. 75, 1996, pp. 1497-1502.

[11] D. Mareci, D. Sutiman, A. Cailean , et al., “Comprative corrosion study of Ag-Pd and Co-Cr alloys used in dental application”, B. Mater. Sci., Vol. 33, 2010, pp 491-500.

[12] S.P. Dimitrijević, B.D. Vurdelja, S.B. Dimitrijević, F.M. Veljković, Z.J. Kamberović, and S.R. Veličković, “Complementary methods for characterization of the corrosion products on the

surface of Ag60Cu26Zn14 and Ag58. 5Cu31. 5Pd10 brazing alloys", Corrosion Reviews, Vol. 38(2), 2020, pp. 111-125.

[13] R.K. Choudhary, A. Laik, P. Mishra, "Microstructure evaluation during stainless-steel copper vacuum brazing with a Ag-Cu-Pd filler alloy: effect of nickel plating", J. Mater. Eng. Perform., Vol. 26, 2017, pp. 1085-1100.

[14] M.M. Mcdonald, D.L. Keller,C.R. Heiple, et al., "wettability of brazing filler metals on molybdenum and TZM", Weld. Res., 1989, pp. 389-395.

[15] H.J. Seol, D.H. Lee, H.K. Lee, et al., "Age-hardening and related phase transformation in an experimental Ag–Cu–Pd–Au alloy", J. Alloys compd., 2006;407:182-187.

[16] Chin HY, Park MG, Kwon YH, et al. Phase transformation and microstructural changes during ageing process of an Ag–Pd–Cu–Au alloy alloy. J. Alloy. compd., Vol. 460, 2008, pp. 331-336.

[17] H.J. Seol, T. Shiraishi, Y. Tanaka, et al. "Effects of Zn addition to AuCu on age-hardening behaviors at intraoral temperature", J. Mater. Sci-Mater. M., Vol. 13, 2013, pp. 237-241.

[18] D. Gheorghe, I. Pencea, I.V. Antoniac, and R.N. Turcu, "Investigation of the Microstructure, Hardness and Corrosion Resistance of a New 58Ag24Pd11Cu2Au2Zn1.5In1.5Sn Dental Alloy Materials, Vol 12(24), 2019, pp. 4199-4112.

[19] G.W. Marshall, S.J. Marshall, K. Szurgot, et al., "Properties of Ag-Cu-Pd dispersed Phase amalgams: microstructures" J. Dent. Res., Vol. 61, 1982, pp. 802-806.

[20] H.J. Seol, T. Shiraishi, Y. Tanaka, et al. "Ordering behaviors and age-hardening in experimental AuCu–Zn pseudobinary alloys for dental applications", Biomaterials, Vol. 23, 2002, pp. 4873-4879.

[21] H. Winn, Y. Tanaka, T. Shiraishi, et al. "Coherent phase diagram of Au–Cu–Pd ternary system near and within the two-phase region of Au Cu and AuCu I ordered phases", J. Alloys compd., Vol. 308, 2000, pp. 269-274.

[22] H.K. Lee, H.M. Moon, H.J. Seol, et al., "Age hardening by dendrite growth in a low-gold dental casting alloy", Biomaterials, Vol. 25, 2004, pp. 3869-3875.

[23] R.G. Davies, N.S. Stoloff, "Order and domain Hardening in Cu_3Au type superlattice alloys", Acta Metall. Vol. 11, 1963, pp. 1347-1353.

[24] K. Yasuda, H. Metahi, Y. Kanzawa, "Structure and morphology of an age-hardened gold-copper-silver dental alloy", J. Less-Com Met., Vol. 60, 1978, pp. 65-78.

[25] M.N. Samani, A. Shokuhfar, A.R. Kamali, M. Hadi, "Production of a nanocrystalline Ni_3Al-based alloy using mechanical alloying", Vol. 500 (1), 2010, pp. 30-33

[26] K. Yasuda, "Age-hardening characteristics of a commercial Dental Gold alloys", J. Less-Com Met., Vol. 70, 1980, pp. 75-87.

[27] M. Nakagawa, K. Yasuda, "Age-hardening and the associated phase transformation in an Au-55.2at% Cu-17.4at% Ag ternary alloy", J. Mater. Sci., Vol. 23, 1988, pp. 2975-2982.